

Design, Synthesis, and Biological Evaluation of Conformationally Restricted Rivastigmine Analogues

Maria Laura Bolognesi, Manuela Bartolini, Andrea Cavalli, Vincenza Andrisano, Michela Rosini, Anna Minarini, and Carlo Melchiorre*

Department of Pharmaceutical Sciences, University of Bologna, Via Belmeloro 6, 40126 Bologna, Italy

Received March 19, 2004

Rivastigmine (**1**), an acetylcholinesterase (AChE) inhibitor approved in 2000 for the treatment of Alzheimer disease, bears a carbamate moiety in its structure, which is able to react covalently with the active site of the enzyme. Kinetic and structural studies on the interaction of **1** with different cholinesterases have been published, giving deeper, but not definitive, insights on the catalysis mechanism. On the basis of these findings and in connection with our previous studies on a series of benzopyrano[4,3-*b*]pyrrole carbamates as AChE inhibitors, we designed a series of conformationally restricted analogues of **1** by including the dimethylamino- α -methylbenzyl moiety in different tricyclic systems. A superimposition between the conformation of **1** and the carbon derivative **4**, as obtained from Monte Carlo simulations, supported the idea that the tricyclic derivatives might act as rigid analogues of **1**. The biological profile of **4–9**, assessed in vitro against human AChE and BChE, validated our rational design. Compound **5**, bearing a sulfur-containing system, showed the highest inhibitory activity, being 192-fold more potent than **1**. In the present study, the most potent inhibitors were always methyl derivatives **3–5**, endowed with a nanomolar range potency, whereas the ethyl ones were 40 times less potent. A reasonable explanation for this finding might be a steric hindrance effect between the ethyl group of **1** and His440 in the active site, as already suggested by the crystal structure of the complex AChE/**1**. The unfavorable influence of the carbamic *N*-alkyl chain on AChE inhibition is less striking when considering BChE inhibition, since BChE is characterized by a bigger acyl binding pocket than AChE. In fact, methyl carbamates **3–5** did not show AChE/BChE selectivity, whereas compounds **6–9** were significantly more potent in inhibiting BChE than AChE activity. At 100 μ M, **5** was found to inhibit the AChE-induced aggregation only by 19% likely because it is not able to strongly interact with the peripheral anionic site of AChE, which plays an essential role in the A β aggregation mediated by the enzyme but is lacking in BChE structure.

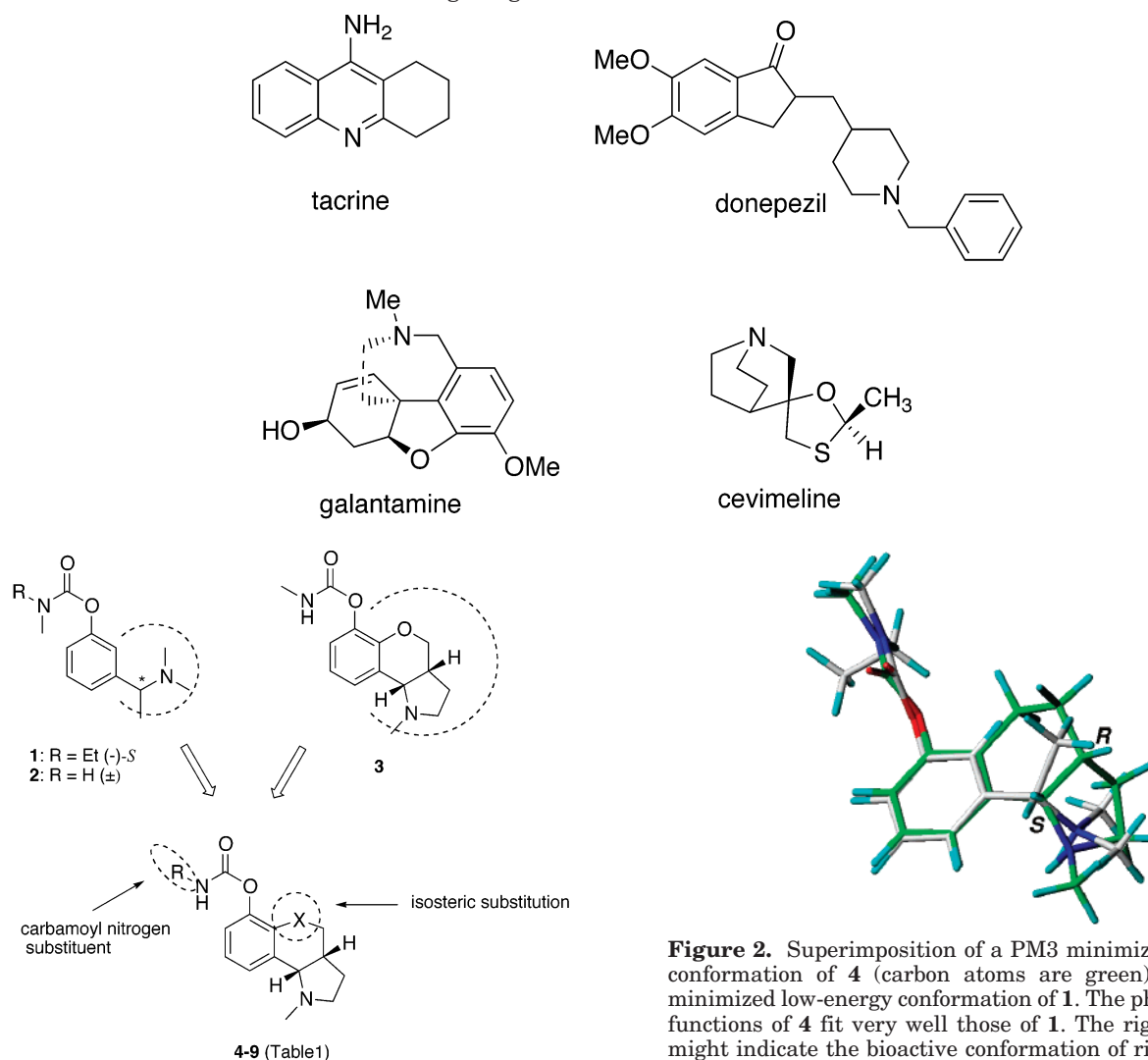
Introduction

Alzheimer's disease (AD), the most common cause of dementia, is a complex neurological affection that is clinically characterized by loss of memory and progressive deficits in different cognitive domains. The consistent neuropathologic hallmark of the disorder, generally noted on postmortem brain examination, is a massive deposit of aggregated protein breakdown products, amyloid plaques, and neurofibrillary tangles. Even if the primary cause of AD is still speculative, the amyloid plaques are thought to be mainly responsible for the devastating clinical effects of the disease.¹ In recent years, significant research attention has also been devoted to the role of free radical formation, oxidative cell damage, and inflammation in the pathogenesis of AD, providing new promising targets and validated animal models.² To date, however, the enhancement of the central cholinergic function is the only clinical effective approach.^{3,4} The intensive research of drugs able to improve the cholinergic transmission in AD has produced so far five launched products, the acetylcholinesterase (AChE) inhibitors tacrine,⁵ donepezil,⁶ rivastigmine, and galantamine,⁷ and the muscarinic

cholinergic agonist cevimeline,⁸ prescribed in the U.S. and Japan for Sjogren's syndrome and currently in clinical trial for AD (Chart 1).

Rivastigmine (**1**, Figure 1), in particular, represents a newer-generation inhibitor,⁹ approved in 2000 under the name of Exelon, endowed with a carbamate structure that makes it a slow substrate able to react covalently with the active site of the enzyme. It belongs to a series of miotine (**2**, Figure 1) derivatives,¹⁰ all of which display inhibitory action toward AChE, but **1** was selected for clinical trials because of its 10-fold greater affinity for brain monomeric G1 over the peripheral form of the enzyme, its chemical stability, and good tolerability. In addition, **1** has an "in vivo" peculiar pharmacological profile;¹¹ it shows interesting selectivity for the brain regions more affected by the neuronal degeneration,¹² has a dual inhibitory action on both AChE and butyrylcholinesterase (BChE), and has demonstrated broad benefits across the severity of AD and also in patients with the Lewy body variant of AD.¹³ Recent evidence suggests that in AD brain, BChE activity rises, while AChE activity remains unchanged or declines. Therefore, both enzymes are likely involved in regulating acetylcholine (ACh) levels and, consequently, may represent legitimate therapeutic targets for the develop-

* To whom correspondence should be addressed. Phone: +39-051-2099706. Fax: +39-051-2099734. E-mail: carlo.melchiorre@unibo.it.

Chart 1. Chemical Structures of Cholinergic Ligands for the Treatment of AD**Figure 1.** Design strategy for the synthesis of 4–9 by inserting the dimethylaminoethylphenyl moiety of 1 in different tricyclic systems related to 3.

ment of agents such as 1, which, with the ability to inhibit BChE in addition to AChE, should lead to improved clinical outcomes.¹⁴

Recent kinetic and structural studies on the interaction of 1 with different cholinesterases gave deeper, but not definitive, insights into the mechanism of catalysis.¹⁵ On the basis of these findings and in connection with our previous studies¹⁶ on a series of benzopyrano[4,3-*b*]pyrrole carbamates as AChE inhibitors, we designed a series of conformationally restricted analogues of 1 and 2 by including the dimethylamino- α -methylbenzyl moiety in different tricyclic systems related to 3 (Figure 1). To support this basic idea, a superimposition between the conformation of 1 and the carbon derivative 4, as obtained from Monte Carlo simulations, was carried out. Low-energy conformations of each molecule were selected and fitted, as shown in Figure 2. Clearly, the overlap was satisfactory (rmsd = 0.28 Å), confirming that the tricyclic derivatives might act as rigid analogues of 1. Thus, the isosteric replacement of the endocyclic oxygen of 3 with a sulfur or a carbon atom, leading to 4 or 5 respectively, might provide information about the physicochemical requirements of the enzyme

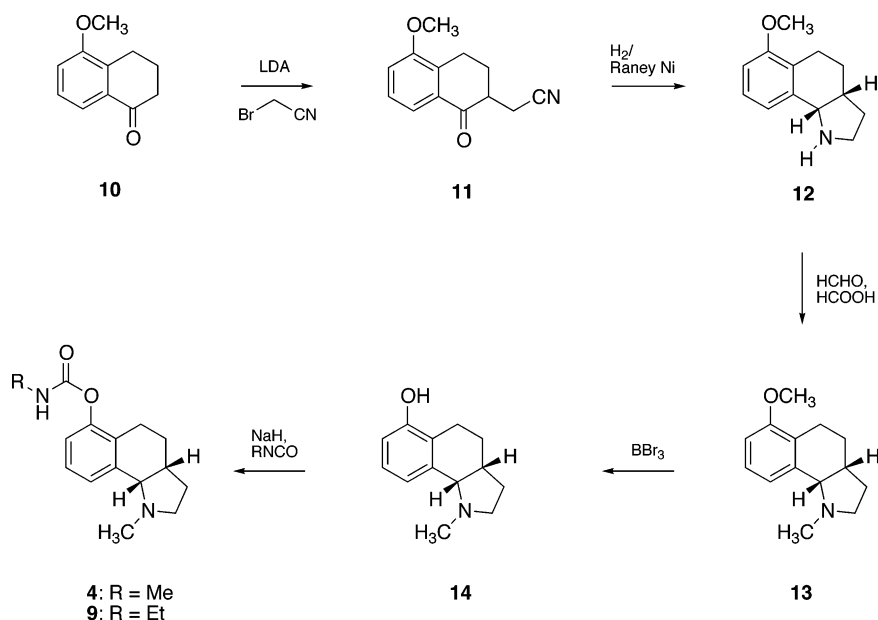
Figure 2. Superimposition of a PM3 minimized low-energy conformation of 4 (carbon atoms are green) onto a PM3 minimized low-energy conformation of 1. The pharmacophoric functions of 4 fit very well those of 1. The rigid analogue 4 might indicate the bioactive conformation of rivastigmine.

binding site, which are still in debate. In addition, the role of the carbamoyl nitrogen substituent of 3 was investigated through the synthesis of different aryl and alkyl carbamates (6–9).

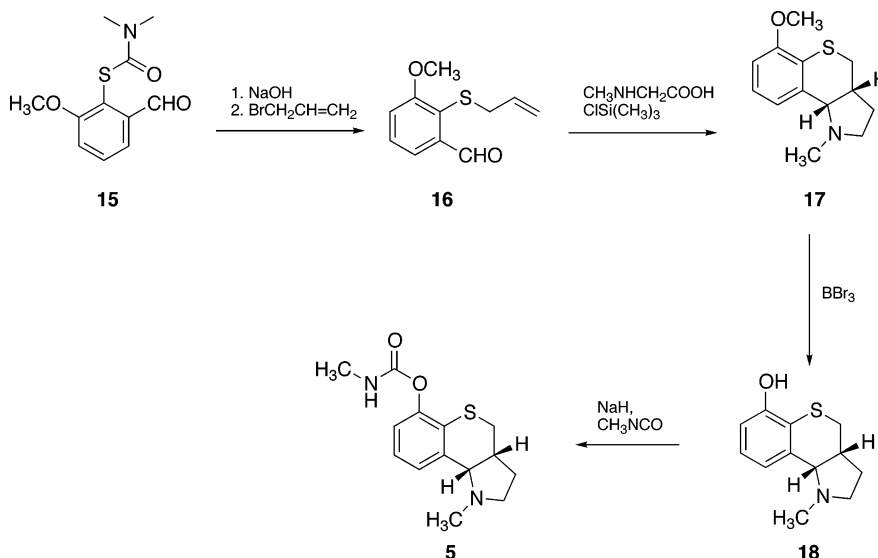
Chemistry

Aryl-functionalized tricyclic pyrrolidines have very few synthetic precedents in the literature,¹⁷ so the development of an efficient synthesis for target compounds 4 and 5 appealed to us. The previous pathway to 3, which involved a [3 + 2] dipolar cycloaddition of a 2-allyloxybenzaldehyde, was not deemed practical for the synthesis of the carbon analogue 4, since the preparation of the corresponding 2-butenylbenzaldehyde was not as feasible. Thus, a different synthetic strategy starting from the commercially accessible tetralone 10 was followed (Scheme 1). Alkylation of the lithium salt of 5-methoxytetralone with bromoacetonitrile in rigorously anhydrous conditions furnished nitrile 11, which in turn was cyclized to 12 through catalytic hydrogenation over Raney Ni.¹⁸ The coupling constant observed for the ring-fusion protons ($J = 6.5$ Hz) was consistent with the reported value for cis isomer 3,¹⁶ and the cis stereochemistry was further secured from detailed nuclear Overhauser effect (NOE) studies. Methylation of the amine function of 12 and subsequent dealkylation

Scheme 1



Scheme 2



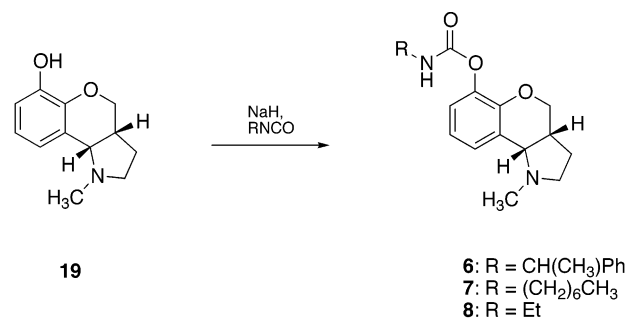
of the methoxy group of **13** gave phenol **14**, which upon reaction with the appropriate isocyanate afforded final compounds **4** and **9**.

In contrast, the synthesis of **5** (Scheme 2) could be performed using the strategy previously described for **3**,¹⁶ through reaction of the key intermediate 2-allylsulfanyl-3-methoxybenzaldehyde (**16**) and sarcosine trimethylsilyl ester. The preparation of **16** was readily accomplished in one pot by sequential treatment of **15**^{19,20} with sodium hydroxide and allyl bromide. After formation of the tricyclic derivative **17**, the synthesis proceeded as depicted for **4** in Scheme 1 and, in agreement with the parent system, the *cis* fusion ring was assigned through the coupling constant of the benzylic methine proton.

Finally, carbamoylation of **19** to give the different carbamates **6–8** was accomplished as reported for the preparation of **4** (Scheme 3).

It should be mentioned that the enantiomer separation of the different racemic mixtures was not per-

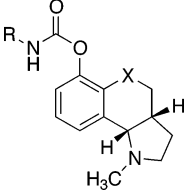
Scheme 3



formed, since we¹⁶ and others²¹ have noticed that the chirality does not seem to strongly affect the inhibitory activity of this class of 1-related compounds.

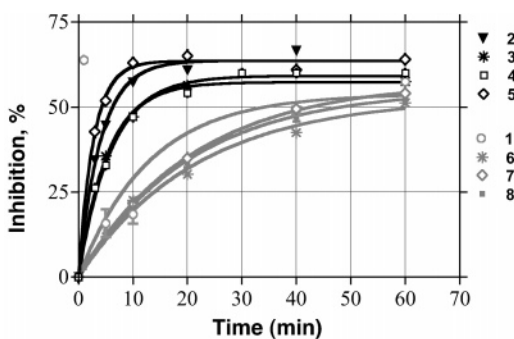
Biology

To determine the potential interest of compounds **4–9** for the treatment of AD, their AChE inhibitory activity

Table 1. Inhibition of AChE and BChE Activities by 1-Related Compounds


compd	X	R	IC ₅₀ ± SEM (nM) ^a	
			AChE	BChE
1	rivastigmine		1535 ± 64	301 ± 14
2	miotine		100 ± 33	406 ± 13
3	O	Me	30.0 ± 1.7	59.4 ± 2.3
4	CH ₂	Me	17.3 ± 1.2	24.5 ± 1.6
5	S	Me	8.11 ± 0.28	10.5 ± 0.5
6	O	CH(CH ₃)Ph	1870 ± 230	209 ± 3
7	O	(CH ₂) ₆ CH ₃	20.3 ± 3.1	1.26 ± 0.04
8	O	Et	420 ± 5	44.41 ± 1.8
9	CH ₂	Et	393 ± 33	30.3 ± 2.5

^a Human recombinant AChE and BChE from human serum were used. IC₅₀ values represent the concentration of inhibitor required to decrease enzyme activity by 50% and are the mean of two independent measurements, each performed in triplicate. The incubation time was between 20 and 60 min, according to the kinetic type.

**Figure 3.** Time course of AChE inhibition at IC₅₀ concentrations for compounds 1–8.

was determined by the method of Ellman et al.²² on human recombinant AChE. Furthermore, to establish the selectivity of 4–9, their BChE inhibitory activity was also calculated by the same method on BChE from human serum. The inhibitory potency was expressed as IC₅₀, which represents the concentration of inhibitor required to decrease the enzyme activity by 50%. To allow comparison of the results, 1–3 were used as the reference compounds.

Finally, the ability of 5 to inhibit the proaggregating action of AChE toward β -amyloid ($A\beta$) was assessed through a thioflavin T-based fluorometric assay,²³ in comparison with 1.

Results and Discussion

The inhibitory potency, expressed as IC₅₀ values, of compounds 4–9 of AChE and BChE is reported in Table 1 in comparison with that of analogue 3 and the two reference compounds 1 and 2. The overlaid time course of inhibition experiments at the IC₅₀ concentrations of inhibitors 1–8 is shown in Figure 3.

The most interesting finding is that the potency toward AChE is generally increased in the rigidified [1]-benzopyrrolo[4,3-*b*]pyrrole derivatives compared to the flexible prototype 1. In particular, derivatives 4, 5, and

7 turned out to be significantly more potent than both rivastigmine (1) and the parent derivative miotine (2), confirming the rational design carried out. Among the restricted analogues, 5 showed the most high inhibitory activity, being 192- and 12-fold more potent than 1 and 2, respectively. A reasonable explanation for this phenomenon is that the tricyclic system of the rigid series acts as a conformationally restricted mimic of the 3-[1-(dimethylamino)ethyl]phenyl fragment of 1, as revealed by Monte Carlo conformational analyses. Actually, 1 displayed as many as 29 low-energy conformations (within an energy window of 3 kcal/mol from the global minimum), whereas the rigid carbon analogue 4 adopted only two possible low-energy conformations. In this respect, the conformation of 4, shown in Figure 2, might indicate the bioactive conformation of 1. The restricted compounds have higher affinity because they do not incur the entropic penalty experienced when 1 and 2, having a freely rotating skeleton, bind.

However, it is well established that several structural elements determine AChE inhibitory activity of carbamate derivatives. For instance, the alkyl substituent on the carbamoyl nitrogen strongly affects the affinity profile. In our series of rigid compounds, the most potent inhibitors resulted in methyl derivatives 3–5, all endowed with potency in the nanomolar range. Increasing the length of the alkyl chain to ethyl resulted in a 40-fold reduction in both the oxygen and carbon series (3 vs 8 and 4 vs 9). A similar behavior was shown by 6, carrying a bulky *R*-1-phenylethyl carbamate on the [1]-benzopyrrolo[4,3-*b*]pyrrole scaffold. The potency was restored to a value similar to that of the methyl derivative 3 by lengthening the chain to *n*-heptyl, affording 7, which displayed an IC₅₀ value of 20.3 nM. These results are in good agreement with the higher potency reported for monosubstituted carbamate derivatives of 1 carrying a methyl group instead of an ethyl one.^{21,24} The anomalous ethyl effect was also observed by Lieske and co-workers,²⁵ who found, in a series of indolyl carbamates, the diethyl derivative to be about 7400-fold less potent than the dimethylcarbamoyl analogue. Actually, to support these experimental data, the crystal structure of AChE/rivastigmine complex has disclosed a steric hindrance effect between the ethyl group of 1 and His440 in the active site, causing a significant movement of this amino acid away from its normal partner, Glu327, and resulting in the disruption of the catalytic triad.¹⁵ However, the high affinity displayed by 7 is not in line with a negative steric effect between the *N*-alkyl substituent of the inhibitor and His440 of the enzyme. Clearly, the *n*-heptyl group of 7 interacts in such a way that the catalytic triad of the active site of AChE is not negatively affected as one would expect simply on the basis of steric hindrance.

The results at BChE had a potency trend similar to that observed at AChE: rigid carbamates 3–5 were 1 order of magnitude more potent than flexible compounds 1 and 2 but, unlike 1 which displayed a preferential BChE selectivity, showed similar IC₅₀ values for AChE and BChE inhibition. Recent evidence suggests that beyond the regulation of synaptic ACh levels BChE may also have a role in the etiology and progression of AD. Consequently, the new compounds, which have a dual

inhibitory action on both AChE and BChE, might show a better therapeutic profile in AD and related dementia.¹⁴ The unfavorable effect of the carbamic *N*-alkyl chain on AChE inhibition was reversed when considering BChE inhibition, as revealed by comparing the IC₅₀ values of the bulky derivatives **6**–**9** for the two enzymes. A reasonable explanation might be that BChE is characterized by a bigger acyl binding pocket than AChE,²⁶ thus accounting for the lower clash effect of a wider substituent toward BChE.

Exchanging the oxygen or the carbon atom with a sulfur (**5** vs **3** and **4**) resulted in a slight increase of both AChE and BChE inhibition, suggesting a favorable short-range interaction between the aromatic moiety of Trp86 (AChE) and Trp82 (BChE) of the active sites and the sulfur atom of the inhibitor.²⁷

The lack of AChE/BChE selectivity is consistent with the finding that our inhibitors weakly prevented the proaggregating effect of AChE toward A β in a thioflavin T-based fluorometric assay previously reported.^{23,28} At 100 μ M, **5** was found to inhibit the AChE-induced aggregation only by 19% likely because it is not able to strongly interact with the peripheral anionic site (PAS) of AChE, which plays an essential role in A β aggregation mediated by the enzyme, whereas it is lacking in BChE. In this respect, docking simulations, purposely addressed to identify a possible binding mode of **5** toward PAS of AChE, turned out to be unable to establish a univocal binding mode, as a possible consequence of the quite low affinity of present inhibitors toward this site. In contrast, **1**, which showed a slightly higher affinity for BChE, was completely unable to act as a proaggregating inhibitor (<5% inhibition at 100 μ M), whereas **5** showed a slightly higher affinity for AChE and a weak effect against the proaggregating activity of AChE. Inhibitors able to bind to both sites of AChE are usually weaker inhibitors of BChE and more potent inhibitors for the proaggregating effect induced by AChE, suggesting that AChE/BChE selectivity might be relevant to establish the capability of a new molecule to contrast A β aggregation.²⁹

Experimental Section

Chemistry. Melting points were taken in glass capillary tubes on a Büchi SMP-20 apparatus and are uncorrected. IR, electron impact (EI) mass spectra, and direct infusion ESI mass spectra were recorded on Perkin-Elmer 297, VG 7070E, and Waters ZQ 4000 apparatus, respectively. ¹H NMR and COSY experiments were recorded on Mercury 400, Varian VXR 200, and Varian VXR 300 instruments. Chemical shifts are reported in parts per million (ppm) relative to tetramethylsilane (TMS), and spin multiplicities are given as s (singlet), br s (broad singlet), d (doublet), t (triplet), or m (multiplet). Although the IR spectral data are not always included (because of the lack of unusual features), they were obtained for all compounds reported and were consistent with the assigned structures. The elemental compositions of the compounds agreed to within $\pm 0.4\%$ of the calculated value. When the elemental analysis is not included, crude compounds were used in the next step without further purification. Chromatographic separations were performed on silica gel columns by flash (Kieselgel 40, 0.040–0.063 mm; Merck) or gravity column (Kieselgel 60, 0.063–0.200 mm; Merck) chromatography. Compounds were named following IUPAC rules as applied by Beilstein-Institut AutoNom (version 2.1), a PC integrated software package for systematic names in organic chemistry. Miotine³⁰ (**2**) and dimethylthiocarbamic acid *S*-(2-formyl-6-

methoxyphenyl) ester (**15**)^{19,20} were prepared according to literature methods.

(5-Methoxy-1-oxo-1,2,3,4-tetrahydronaphthalen-2-yl)-acetonitrile (11). A solution of 1.6 *N n*-butyllithium (6.87 mL, 0.011 mol) in hexane was slowly added to a cold (–60 °C) solution of diisopropylamine (1.68 mL, 0.011 mol) in dry THF (5 mL). After 0.5 h, a solution of 5-methoxytetralone (1.76 g, 0.010 mol) in THF (2 mL) was added dropwise, followed by the addition of bromoacetonitrile (0.77 mL, 0.011 mol). The temperature was allowed to warm from –60 °C to room temperature, and the reaction mixture was stirred for 16 h. It was diluted with water and extracted with EtOAc. The organic layer was dried and concentrated to give a brown oily residue, which was purified by flash chromatography. Eluting with petroleum ether/EtOAc (8.5:1.5), the second fraction corresponded to **11** (230 mg, 11% yield) as clear solid: mp 104–105 °C; EI-MS *m/z* = 215 (M⁺); IR ν_{\max} 2238 cm^{–1} (CN); ¹H NMR (CDCl₃, 200 MHz) δ 7.65 (d, 1H), 7.31 (t, 1H), 7.07 (d, 1H), 3.89 (s, 3H), 3.35–3.20 (dq, 1H), 3.08–2.98 (dd, 1H), 2.95–2.75 (m complex, 2H), 2.70–2.45 (m complex, 2H), 2.10–1.85 (m, 1H); ¹³C (CDCl₃, 200 MHz) δ 195.99, 156.56, 132.58, 132.34, 127.10, 118.80, 118.45, 114.57, 77.63, 77.00, 76.37, 55.63, 43.87, 27.89, 22.41, 18.25.

cis-6-Methoxy-2,3,3a,4,5,9b-hexahydro-1H-benzo[g]indole (12). A solution of **11** (230 mg, 1.07 mmol) in absolute EtOH (15 mL) was hydrogenated in the presence of Raney nickel (0.2 g) at atmospheric pressure and room temperature for 2 days. The mixture was filtered through Celite, and the filtrate was evaporated to give a residue, which was purified by flash chromatography. Eluting with CH₂Cl₂/MeOH/NH₃ (9.5:0.5:0.05) afforded **12** (100 mg, 46% yield) as brown oil: ¹H NMR (CDCl₃, 400 MHz) δ 7.15 (t, 1H), 7.07 (d, 1H), 6.72 (d, 1H), 4.07 (d, 1H), 3.84 (br s, 1H exch), 3.80 (s, 3H), 3.20–3.08 (m, 1H), 2.85–3.00 (m + td, 1H + 1H), 2.45–2.30 (m complex, 2H), 2.20–2.10 (m, 1H), 1.78–1.73 (m, 1H), 1.70–1.60 (m, 1H), 1.45–1.35 (dq, 1H).

cis-6-Methoxy-1-methyl-2,3,3a,4,5,9b-hexahydro-1H-benzo[g]indole (13). Formic acid (96%, 2.01 mL, 17.4 mmol) was added dropwise to **12** (100 mg, 0.49 mmol), and then formaldehyde (37%, 1.8 mL) was added to the resulting mixture, which was heated at 90 °C for 10 h, cooled (0 °C), diluted with water, and washed with CH₂Cl₂. The aqueous layer was then made basic with aqueous 40% NaOH and extracted with CH₂Cl₂ (4 \times). Removal of the dried solvents gave a residue, which was purified by flash chromatography. Eluting with CH₂Cl₂/MeOH/NH₃ (9.3:0.7:0.07) afforded **13** (70 mg, 65% yield) as a clear oil: ¹H NMR (CDCl₃, 200 MHz) δ 7.28–7.12 (m, 1H), 6.84–6.78 (m, 2H), 3.83 (s, 3H), 3.15–3.05 (m + d, 1H + 1H), 2.86–2.61 (m complex, 2H), 2.59–2.43 (m, 1H), 2.36 (s, 3H), 2.31–2.21 (m, 1H), 2.15–2.00 (m, 1H), 1.86–1.52 (m, 3H).

cis-1-Methyl-2,3,3a,4,5,9b-hexahydro-1H-benzo[g]indol-6-ol (14). A sample of 1 M BBr₃ in CH₂Cl₂ (2 mL) was added to a stirred and cooled (0 °C) solution of **13** (70 mg, 0.32 mmol) in anhydrous CHCl₃ (4 mL) under a stream of dry nitrogen. When the addition was completed, the reaction mixture was stirred at room temperature for 4 h. After the mixture was cooled at 0 °C, excess BBr₃ was destroyed by cautious dropwise addition of anhydrous MeOH (10 mL). The resulting mixture was heated at reflux for 2 h. Removal of the solvent gave a viscous solid, which was purified by flash chromatography. Eluting with CH₂Cl₂/MeOH/NH₃ (9.6:0.4:0.04) afforded **13** (50 mg, 77% yield) as a clear oil: ¹H NMR (CDCl₃, 200 MHz) δ 6.83 (t, 1H), 6.65 (d, 1H), 6.33 (d, 1H), 5.32 (br s, 1H exch), 3.20 (m + d, 1H + 1H), 2.78–2.53 (m complex, 3H), 2.49 (s, 3H), 2.43–2.29 (m, 1H), 2.13–1.96 (m, 1H), 1.92–1.70 (m complex, 2H), 1.61–1.43 (m, 1H).

cis-Methylcarbamic Acid 1-Methyl-2,3,3a,4,5,9b-hexahydro-1H-benzo[g]indol-6-yl Ester Hydrochloride (4). MeNCO (4 μ L, 0.068 mol) was added to a stirred mixture of **14** (10 mg, 0.050 mmol) and NaH (1 mg, 0.044 mmol) in anhydrous THF (2 mL). Stirring was continued for 20 h at room temperature, and then removal of the solvent gave a residue that was transformed into the hydrochloride salt: 80% yield; mp 180–

183 °C (from EtOH/ether); MS (ESI⁺) $m/z = 261.2 (M + H)^+$; ¹H NMR (CD₃OD, 300 MHz) δ 7.45–7.39 (m, 2H), 7.21 (t, 1H), 4.55 (d, 1H), 3.84–3.71 (m, 1H), 3.40–3.25 (m, 1H), 3.04 (s, 3H), 3.00–2.84 (m, 1H), 2.80 (s, 3H), 2.75 (t, 2H), 2.61–2.41 (m, 1H), 2.10–1.90 (m, 1H), 1.89–1.70 (m, 2H). Anal. (C₁₅H₂₁ClN₂O₂) C, H, N.

2-Allylsulfanyl-3-methoxybenzaldehyde (16). A solution of **15** (2.80 g, 0.012 mol) in MeOH (11 mL) was stirred under reflux under nitrogen for 1 h with aqueous 10% NaOH (5.6 mL, 0.014 mol). The cooled alkaline mixture was then treated with a solution of allyl bromide (1.12 mL, 0.013 mol) in MeOH (25 mL) and stirred at room temperature overnight. The formed white solid was filtered off, and the filtrate evaporated to give a residue, which was purified by flash chromatography. Eluting with petroleum ether/EtOAc (9:1) afforded **16** as brown oil: 65% yield; ¹H NMR (CDCl₃, 300 MHz) δ 10.72 (s, 1H), 7.51 (d, 1H), 7.40 (t, 1H), 7.11 (d, 1H), 5.80–5.60 (m, 1H), 4.88–4.80 (m, 2H), 3.95 (s, 3H), 3.47 (d, 2H).

cis-6-Methoxy-1-methyl-1,2,3,3a,4,9b-hexahydro-5-thia-1-azacyclopenta[*a*]naphthalene (17). A mixture of *N*-methylglycine (2.13 g, 0.024 mol) and chlorotrimethylsilane (30.3 mL, 2.39 mmol) was gently refluxed under nitrogen for 3 h. After the mixture was cooled, the formed solid was collected by filtration and washed with dry ether. To a suspension of this solid in dry toluene (70 mL) were added diisopropylethylamine (6.56 mL, 37.7 mmol) and **16** (1.35 g, 6.5 mmol), the reaction mixture was heated under reflux, and the water that was formed continuously was removed for 18 h. Removal of the solvent gave an oil that was partitioned between aqueous NaHCO₃ and CH₂Cl₂. The organic phase was dried and evaporated to give a residue that was purified by flash chromatography. Eluting with petroleum ether/EtOAc/MeOH/NH₃ (8:1.5:0.5:0.05) afforded **17** as a clear oil: 60% yield; ¹H NMR (CDCl₃, 300 MHz) δ 7.11 (t, 1H), 6.84–6.78 (m, 2H), 3.89 (s, 3H), 3.18–3.10 (d + m, 2H), 3.00–2.80 (m, 1H), 2.74 (d, 2H), 2.30–2.20 (s + m, 3H + 1H), 2.12–2.02 (m, 2H).

cis-1-Methyl-1,2,3,3a,4,9b-hexahydro-5-thia-1-azacyclopenta[*a*]naphthalen-6-ol (18). It was synthesized from **17** (400 mg, 0.017 mol) following the procedure described for **14**: 60% yield; EI-MS $m/z = 221 (M^+)$; ¹H NMR (CDCl₃, 200 MHz) δ 7.10 (t, 1H), 6.90–6.77 (m, 2H), 4.85 (br s, 1H exch), 3.21–3.14 (d + m, 2H), 3.14–2.90 (m, 1H), 2.79–2.59 (m, 2H), 2.34–2.20 (s + m, 4H), 2.19–2.05 (m, 2H).

cis-Methylcarbamic Acid 1-Methyl-1,2,3,3a,4,9b-hexahydro-5-thia-1-azacyclopenta[*a*]naphthalen-6-yl Ester Hydrochloride (5). It was synthesized from **18** (95 mg, 0.43 mmol) following the procedure described for **4**: 40% yield; mp 202–206 °C; ¹H NMR (free base, CDCl₃, 200 MHz) δ 7.20–7.00 (m, 3H), 5.20 (br s, 1H exch), 3.20–3.10 (d + m, 2H), 3.00–2.80 (d + m, 4H), 2.80–2.60 (m, 2H), 2.40–2.20 (s + m, 3H + 1H), 2.15–1.15 (m, 2H). Anal. (C₁₄H₁₉ClN₂O₂S) C, H, N.

cis-*R*-(1-Phenylethyl)carbamic Acid 1-Methyl-1,2,3,3a,4,9b-hexahydro-5-oxa-1-azacyclopenta[*a*]naphthalen-6-yl Ester Hydrochloride (6). It was synthesized from **19**¹⁶ (70 mg, 0.34 mmol) and *R*-(+)-1-phenylethyl isocyanate following the procedure described for **4**: 80% yield; mp 196–200 °C; EI-MS $m/z = 352 (M^+)$; ¹H NMR (free base, CDCl₃, 300 MHz) δ 7.40–7.20 (m, 5H), 7.10–6.95 (d, 2H), 7.85 (t, 1H), 5.35 (br s, 1H exch), 5.00–4.90 (m, 1H), 4.10–4.00 (m, 1H), 4.95–4.80 (t, 1H), 3.10–3.00 (t, 1H), 3.00–2.90 (d, 1H), 2.40–2.25 (s + q, 5H), 2.10–2.00 (m, 1H), 1.60–1.40 (d + m, 4H); ¹H NMR (CD₃OD, 300 MHz) δ 8.15 (br s, 1H exch), 7.37–7.26 (m, 5H), 7.25–7.18 (m, 2H), 7.10–7.05 (t, 1H), 4.90–4.70 (m, 1H), 4.70–4.50 (m, 1H), 4.15–4.00 (m, 1H), 3.95–3.80 (m, 1H), 3.75–3.60 (m, 1H), 3.06 (s + m, 3H + 2H), 2.60–2.40 (m, 1H), 2.10–1.90 (m, 1H), 1.49 (d, 3H). Anal. (C₂₁H₂₅ClN₂O₂) C, H, N.

cis-Heptylcarbamic Acid 1-Methyl-1,2,3,3a,4,9b-hexahydro-5-oxa-1-azacyclopenta[*a*]naphthalen-6-yl Ester Hydrochloride (7). It was synthesized from **19**¹⁶ (90 mg, 0.44 mmol) and heptyl isocyanate following the procedure described for **4**: 79% yield; mp 160–161 °C; ¹H NMR (free base, CDCl₃, 200 MHz) δ 7.10–7.03 (m, 2H), 6.89 (t, 1H), 5.09 (br s, 1H

exch), 4.13–4.06 (m, 1H), 3.92 (t, 1H), 3.24 (q, 2H), 3.14–3.05 (m, 1H), 2.97 (d, 1H), 2.50–2.35 (s + m, 3H + 1H), 2.34 (q, 1H), 2.18–2.00 (m, 1H), 1.60–1.20 (m complex, 11H), 0.91 (t, 3H). Anal. (C₂₀H₃₁ClN₂O₃) C, H, N.

cis-Ethylcarbamic Acid 1-Methyl-1,2,3,3a,4,9b-hexahydro-5-oxa-1-azacyclopenta[*a*]naphthalen-6-yl Ester Hydrochloride (8). It was synthesized from **19**¹⁶ (100 mg, 0.49 mmol) and ethyl isocyanate following the procedure described for **4**: 52% yield; mp 176 °C dec; ¹H NMR (free base, CDCl₃, 200 MHz) δ 7.09–7.02 (m, 2H), 6.91 (t, 1H), 5.12 (br s, 1H exch), 4.13–4.05 (m, 1H), 3.91 (t, 1H), 3.39–3.25 (m, 2H), 3.14–3.04 (m, 1H), 2.97 (d, 1H), 2.55–2.38 (m + s, 3H + 1H), 2.32 (q, 1H), 2.14–1.98 (m, 1H), 1.55–1.39 (m, 1H), 1.27–1.15 (m, 3H). Anal. (C₁₅H₂₁ClN₂O₃) C, H, N.

cis-Ethylcarbamic Acid 1-Methyl-2,3,3a,4,5,9b-hexahydro-1*H*-benzo[*g*]indol-6-yl Ester Hydrochloride (9). It was synthesized from **14** (50 mg, 0.25 mmol) and ethyl isocyanate following the procedure described for **4**: 30% yield; EI-MS $m/z = 274 (M^+)$; ¹H NMR (free base, CDCl₃, 200 MHz) δ 7.18 (t, 1H), 7.06–7.01 (m, 2H), 5.04 (br s, 1H exch), 3.39–3.25 (m, 2H), 3.13–3.06 (m, 2H), 2.64–2.51 (m complex, 3H), 2.33–2.21 (s + m, 3H + 1H), 2.15–2.01 (m, 1H), 2.00–1.53 (m complex, 3H), 1.22 (t, 3H). Anal. (C₁₆H₂₃ClN₂O₂) C, H, N.

NMR Analysis. To assign the protons at positions 3a and 9b of the benzindole system, the structure of **12** was determined by 2D ¹H and ¹³C NMR spectroscopy. Irradiation of the doublet signal produced by the hydrogen atom 9b at 4.07 ppm resulted in a positive nuclear Overhauser effect (NOE) in the multiplet corresponding to the 3a proton (2.30–2.34), confirming the *cis* ring fusion. ¹H, ¹³C, and 2D NMR spectra were measured using a 20 mg sample of **12** dissolved in 0.7 mL of CDCl₃ and measured on a Mercury 400 MHz spectrometer at 30 °C.

Biology. Inhibition of AChE and BChE. The method of Ellman et al.²² was followed. **1** was obtained by extraction from Exelon tablets, and the purity was confirmed by HPLC. AChE stock solution was prepared by dissolving 1000 units of lyophilized powder (Sigma Chemical) in 0.1 M phosphate buffer (pH 8.0) containing Triton X-100, 0.1%. BChE stock solution was prepared by dissolving 100 units of lyophilized powder (Sigma Chemical) in aqueous gelatin solution (0.1% w/v). Enzymes stock solutions were diluted before use to reach an activity ranging between 0.13 and 0.100 AU/min in the final assay conditions. Stock solutions of the tested compounds (1 mM) were prepared in methanol. Five different concentrations of each compound were used to obtain inhibition of AChE or BChE activity between 20% and 80%. The assay solution consisted of 0.1 M phosphate buffer (pH 8.0), with the addition of 340 μ M DTNB (Ellman's reagent), AChE or BChE, and 550 μ M acetylthiocholine iodide (ATCh). The final assay volume was 1 mL. Initial rate assays were performed at 37 °C with a Jasco V-530 double beam spectrophotometer: the rate of increase in the absorbance at 412 nm was followed for 5 min. Test compounds were added to the assay solution and preincubated with the enzyme for times between 20 and 60 min, according to the kinetic type, followed by the addition of substrate. Assays were done with a blank containing all components except AChE or BChE to account for nonenzymatic reaction. The reaction rates were compared, and the percent inhibition due to the presence of the test compound was calculated. Each concentration was analyzed in triplicate, and IC₅₀ values were determined graphically from the log concentration–inhibition curves.

Inhibition of AChE Induced A β Aggregation. Thioflavin T (Basic Yellow 1), human recombinant AChE lyophilized powder, 1,1,1,3,3,3-hexafluoro-2-propanol (HFIP), and Triton X-100 were purchased from Sigma Chemicals. Buffers and other chemicals were of analytical grade. Absolute DMSO over molecular sieves was from Fluka. Water was deionized and doubly distilled. A β (1–40), supplied as trifluoroacetate salt, was purchased from Bachem AG. A β (2 mg mL⁻¹) was dissolved in HFIP, lyophilized, and used in this form after dilution for aggregation experiments.

Aliquots of 2 μL of A β peptide, lyophilized from 2 mg mL⁻¹ HFIP solution, and dissolved in DMSO, were incubated for 24 h at room temperature in 0.215 M sodium phosphate buffer (pH 8.0) at a final concentration of 230 μM . For co-incubation experiments aliquots (16 μL) of AChE (final concentration of 2.30 μM , A β /AChE molar ratio of 100:1) and AChE in the presence of 2 μL of the tested inhibitors in 0.215 M sodium phosphate buffer, pH 8.0, solution (final inhibitor concentration ranging between 10 and 250 μM) were added. Blanks containing A β , AChE, and A β , plus inhibitors at 100 μM , in 0.215 M sodium phosphate buffer (pH 8.0) were prepared. The final volume of each vial was 20 μL . Each assay was run in duplicate. To quantify amyloid fibril formation, the thioflavin T fluorescence method was then applied.^{23,31,32} The fluorescence intensities were compared and the percent inhibition due to the presence of test compounds was calculated. The percent inhibition of the AChE induced aggregation due to the presence of the inhibitor was calculated by the following expression: $100 - (\text{IF}_i/\text{IF}_0 \times 100)$ where IF_i and IF_0 are the fluorescence intensities obtained for A β plus AChE in the presence and in the absence of inhibitor, respectively, minus the fluorescent intensities due to the respective blanks.³³

Molecular Modeling. (1) Construction of the Models.

1 and 4 were built by properly modifying the 1-(1-(dimethylamino)ethyl)-7-methyl-8,9-dihydro-7H-5-oxa-7-azabenzocyclohepten-6-one skeleton retrieved from the Cambridge Structural Database (CSD code KEXXUG). The models were minimized first by using steepest descent and then conjugate gradient until a convergence of 0.05 kcal mol⁻¹ Å⁻¹ on the gradient was reached. Then conformational analyses were carried out, and the minimum energy conformers were further optimized at semiempirical Hamiltonian level PM3,³⁴ as implemented in the SYBYL 6.8 (Tripos Inc., St. Louis, MO) graphic interface to MOPAC (keywords PRECISE and MMOK).

(2) Conformational Analyses. Monte Carlo conformational analyses³⁵ were carried out by means of the MacroModel package software,³⁶ using the MMFF force field³⁷ and the generalized Born/surface area (GB/SA) continuum solvation model to simulate the aqueous environment.³⁸ In a Monte Carlo study, the phase space of a molecule is sampled by randomly changing dihedral angle rotations or atom positions. Then the trial conformation is accepted if its energy has decreased from the previous one. If the energy is higher, various criteria can be applied to accept or reject the Monte Carlo trial. In the present simulations, the number of Monte Carlo steps was set equal to 5000 and the trial conformation was accepted if the energy was lower than that of the previous conformation or if its energy was within an energy window of 100 kJ/mol. Then the conformations were grouped by means of a cluster analysis³⁹ using geometrical parameters as filtering screens. The combined use of Monte Carlo and cluster analyses has turned out to be a potent means for sampling the conformational space of highly flexible molecules.⁴⁰

(3) Docking Simulations. To identify the possible binding mode of the compounds at the AChE PAS, 100 docking simulations were performed by means of the DOCK 4.0.1 package software⁴¹ and using the cocrystal between the AChE and Fasciculin (PDB code 1B41).⁴² Fasciculin was removed from the complex, and the truncated residues Glu268, Gln291, Glu369, and Arg522 were properly completed by means of the Biopolymer module of SYBYL 6.8. Hydrogen atoms were added to the protein amino acids, and the atomic partial charges from the all-atom Amber force field were loaded.⁴³

Acknowledgment. This work was supported by grants from the University of Bologna (Funds for Selected Research Topics) and MIUR.

Supporting Information Available: Results from elemental analysis. This material is available free of charge via the Internet at <http://pubs.acs.org>.

References

- Hardy, J.; Selkoe, D. J. The amyloid hypothesis of Alzheimer's disease: progress and problems on the road to therapeutics. *Science* **2002**, *297*, 353–356.

- Capsoni, S.; Ugolini, G.; Comparini, A.; Ruberti, F.; Berardi, N.; Cattaneo, A. Alzheimer-like neurodegeneration in aged antinerve growth factor transgenic mice. *Proc. Natl. Acad. Sci. U.S.A.* **2000**, *97*, 6826–6831.
- Bartus, R. T. On neurodegenerative diseases, models, and treatment strategies: lessons learned and lessons forgotten a generation following the cholinergic hypothesis. *Exp. Neurol.* **2000**, *163*, 495–529.
- Terry, A. V., Jr.; Buccafusco, J. J. The cholinergic hypothesis of age and Alzheimer's disease-related cognitive deficits: recent challenges and their implications for novel drug development. *J. Pharmacol. Exp. Ther.* **2003**, *306*, 821–827.
- Davis, K. L.; Powchik, P. Tacrine. *Lancet* **1995**, *345*, 625–630.
- Bryson, H. M.; Benfield, P. Donepezil. *Drugs Aging* **1997**, *10*, 234–239 (discussion 240–231).
- Sramek, J. J.; Frackiewicz, E. J.; Cutler, N. R. Review of the acetylcholinesterase inhibitor galanthamine. *Expert Opin. Invest. Drugs* **2000**, *9*, 2393–2402.
- Fisher, A.; Pittel, Z.; Haring, R.; Bar-Ner, N.; Kliger-Spatz, M.; Natan, N.; Egozi, I.; Sonego, H.; Marcovitch, I.; Brandeis, R. M1 muscarinic agonists can modulate some of the hallmarks in Alzheimer's disease: implications in future therapy. *J. Mol. Neurosci.* **2003**, *20*, 349–356.
- Gottwald, M. D.; Rozanski, R. I. Rivastigmine, a brain-region selective acetylcholinesterase inhibitor for treating Alzheimer's disease: review and current status. *Expert Opin. Invest. Drugs* **1999**, *8*, 1673–1682.
- Weinstock, M.; Razin, M.; Chorev, M.; Tashma, Z. *Advances in Behavioral Biology*; Plenum Press: New York, 1986; pp 539–551.
- Williams, B. R.; Nazarians, A.; Gill, M. A. A review of rivastigmine: a reversible cholinesterase inhibitor. *Clin. Ther.* **2003**, *25*, 1634–1653.
- Enz, A.; Amstutz, R.; Boddeke, H.; Gmelin, G.; Malanowski, J. Brain selective inhibition of acetylcholinesterase: a novel approach to therapy for Alzheimer's disease. *Prog. Brain Res.* **1993**, *98*, 431–438.
- Bullock, R. The clinical benefits of rivastigmine may reflect its dual inhibitory mode of action: an hypothesis. *Int. J. Clin. Pract.* **2002**, *56*, 206–214.
- Giacobini, E.; Spiegel, R.; Enz, A.; Veroff, A. E.; Cutler, N. R. Inhibition of acetyl- and butyryl-cholinesterase in the cerebrospinal fluid of patients with Alzheimer's disease by rivastigmine: correlation with cognitive benefit. *J. Neural Transm.* **2002**, *109*, 1053–1065.
- Bar-On, P.; Millard, C. B.; Harel, M.; Dvir, H.; Enz, A.; Sussman, J. L.; Silman, I. Kinetic and structural studies on the interaction of cholinesterases with the anti-Alzheimer drug rivastigmine. *Biochemistry* **2002**, *41*, 3555–3564.
- Bolognesi, M. L.; Andrisano, V.; Bartolini, M.; Minarini, A.; Rosini, M.; Tumiatti, V.; Melchiorre, C. Hexahydrochromeno[4,3-*b*]pyrrole derivatives as acetylcholinesterase inhibitors. *J. Med. Chem.* **2001**, *44*, 105–109.
- Hanessian, S.; Papeo, G.; Angiolini, M.; Fettes, K.; Beretta, M.; Munro, A. Synthesis of functionally diverse and conformationally constrained polycyclic analogues of proline and prolinol. *J. Org. Chem.* **2003**, *68*, 7204–7218.
- Gruenfeld, N. Indeno and Naphth[1,2-*d*]azepines. U.S. Patent 4,173,633, 1979.
- Rahaman, L. K. A.; Scrowston, R. M. 7-Substituted Benzo[*b*]thiophenes and 1,2-Benzisothiazoles. Hydroxy- or Methoxy-derivatives. *J. Chem. Soc., Perkin Trans. 1* **1983**, *12*, 2973–2978.
- Yaouancq, L.; Anissimova, M.; Badet-Denisot, M.-L.; Badet, B. Design and Evaluation of Mechanism-Based Inhibitors of D-Alanyl-D-alanine Dipeptidase Van X. *Eur. J. Org. Chem.* **2002**, 3573–3579.
- Sterling, J.; Herzig, Y.; Goren, T.; Finkelstein, N.; Lerner, D.; Goldenberg, W.; Miskolci, I.; Molnar, S.; Rantal, F.; Tamas, T.; Toth, G.; Zagyva, A.; Zekany, A.; Finberg, J.; Lavian, G.; Gross, A.; Friedman, R.; Razin, M.; Huang, W.; Kraiss, B.; Chorev, M.; Youdim, M. B.; Weinstock, M. Novel dual inhibitors of AChE and MAO derived from hydroxy aminoindan and phenethylamine as potential treatment for Alzheimer's disease. *J. Med. Chem.* **2002**, *45*, 5260–5279.
- Ellman, G. L.; Courtney, K. D.; Andres, V., Jr.; Feather-Stone, R. M. A new and rapid colorimetric determination of acetylcholinesterase activity. *Biochem. Pharmacol.* **1961**, *7*, 88–95.
- Bartolini, M.; Bertucci, C.; Cavrini, V.; Andrisano, V. beta-Amyloid aggregation induced by human acetylcholinesterase: inhibition studies. *Biochem. Pharmacol.* **2003**, *65*, 407–416.
- Weinstock, M.; Razin, M.; Chorev, M.; Enz, A. Pharmacological evaluation of phenyl-carbamates as CNS-selective acetylcholinesterase inhibitors. *J. Neural Transm., Suppl.* **1994**, *43*, 219–225.
- Lieske, C. N.; Gepp, R. T.; Clark, J. H.; Meyer, H. G.; Blumbergs, P.; Tseng, C. C. Anticholinesterase activity of potential therapeutic 5-(1,3,3-trimethylindolyl) carbamates. *J. Enzyme Inhib.* **1991**, *5*, 215–223.

- (26) Nicolet, Y.; Lockridge, O.; Masson, P.; Fontecilla-Camps, J. C.; Nachon, F. Crystal structure of human butyrylcholinesterase and of its complexes with substrate and products. *J. Biol. Chem.* **2003**, *278*, 41141–41147.
- (27) Yuan, T.; Weljie, A. M.; Vogel, H. J. Tryptophan fluorescence quenching by methionine and selenomethionine residues of calmodulin: orientation of peptide and protein binding. *Biochemistry* **1998**, *37*, 3187–3195.
- (28) Inestrosa, N. C.; Alvarez, A.; Perez, C. A.; Moreno, R. D.; Vicente, M.; Linker, C.; Casanueva, O. I.; Soto, C.; Garrido, J. Acetylcholinesterase accelerates assembly of amyloid-beta-peptides into Alzheimer's fibrils: possible role of the peripheral site of the enzyme. *Neuron* **1996**, *16*, 881–891.
- (29) Piazzzi, L.; Rampa, A.; Bisi, A.; Gobbi, S.; Belluti, F.; Cavalli, A.; Bartolini, M.; Andrisano, V.; Valenti, P.; Recanatini, M. 3-(4-[[Benzyl(methyl)amino]methyl]phenyl)-6,7-dimethoxy-2H-2-chromenone (AP2238) inhibits both acetylcholinesterase and acetylcholinesterase-induced beta-amyloid aggregation: a dual function lead for Alzheimer's disease therapy. *J. Med. Chem.* **2003**, *46*, 2279–2282.
- (30) Ciszewska, G.; Pfefferkorn, H.; Tang, Y. S.; Jones, L.; Tarapata, R.; Sunay, U. B. Synthesis of tritium, deuterium, and carbon-14 labeled (S)-N-ethyl-N-methyl-3-[1-(dimethylamino)ethyl] carbamic acid, phenyl ester, (L)-2,3-dihydroxybutanedioic acid salt (SDZ ENA 713 hta), an investigational drug for the treatment of Alzheimer's disease. *J. Labelled Compd. Radiopharm.* **1997**, *39*, 651–668.
- (31) Naiki, H.; Higuchi, K.; Nakakuki, K.; Takeda, T. Kinetic analysis of amyloid fibril polymerization in vitro. *Lab. Invest.* **1991**, *65*, 104–110.
- (32) LeVine, H., 3rd Quantification of beta-sheet amyloid fibril structures with thioflavin T. *Methods Enzymol.* **1999**, *309*, 274–284.
- (33) De Ferrari, G. V.; Mallender, W. D.; Inestrosa, N. C.; Rosenberry, T. L. Thioflavin T is a fluorescent probe of the acetylcholinesterase peripheral site that reveals conformational interactions between the peripheral and acylation sites. *J. Biol. Chem.* **2001**, *276*, 23282–23287.
- (34) Stewart, J. P. P. Optimization of parameters for semiempirical methods I. Method. *J. Comput. Chem.* **1989**, *10*, 209–220.
- (35) Chang, G.; Guida, W. C.; Still, W. C. An internal coordinate Monte carlo method for searching conformational space. *J. Am. Chem. Soc.* **1989**, *111*, 4379–4386.
- (36) Mohamadi, F.; Richards, N. G. J.; Guida, W. C.; Liskamp, R. M. J.; Lipton, M.; Caufield, C.; Chang, G. MacroModel—An integrated software system for modeling organic and bioorganic molecules using molecular mechanics. *J. Comput. Chem.* **1990**, *11*, 440–467.
- (37) Halgren, T. A. Merck molecular force field. I. Basis, form, scope, parameterization, and performance of MMFF94. *J. Comput. Chem.* **1996**, *17*, 490–519.
- (38) Still, W. C.; Tempzyk, A.; Hawley, R.; Hendrickson, T. Semi-analytical treatment of solvation for molecular mechanics and dynamics. *J. Am. Chem. Soc.* **1990**, *112*, 6127–6129.
- (39) Shenkin, P. S.; McDonald, D. Q. Cluster analysis of molecular conformations. *J. Comput. Chem.* **1994**, *15*, 899–916.
- (40) Cavalli, A.; Poluzzi, E.; De Ponti, F.; Recanatini, M. Toward a pharmacophore for drugs inducing the long QT syndrome: insights from a CoMFA study of HERG K(+) channel blockers. *J. Med. Chem.* **2002**, *45*, 3844–3853.
- (41) Kuntz, I. D.; Blaney, J. M.; Oatley, S. J.; Langridge, R.; Ferrin, T. E. A geometric approach to macromolecule–ligand interactions. *J. Mol. Biol.* **1982**, *161*, 269–288.
- (42) Kryger, G.; Harel, M.; Giles, K.; Tokar, L.; Velan, B.; Lazar, A.; Kronman, C.; Barak, D.; Ariel, N.; Shafferman, A.; Silman, I.; Sussman, J. L. Structures of recombinant native and E202Q mutant human acetylcholinesterase complexed with the snake-venom toxin fasciculin-II. *Acta Crystallogr., Sect. D: Biol. Crystallogr.* **2000**, *56* (Part 11), 1385–1394.
- (43) Cornell, W. D.; Cieplak, P.; Bayly, C. I.; Gould, I. R.; Merz, K. M.; Ferguson, D. M.; Spellmeyer, D. C.; Fox, T.; Caldwell, J. W.; Kollman, P. A. A second generation force field for the simulation of proteins, nucleic acids, and organic molecules. *J. Am. Chem. Soc.* **1995**, *117*, 5179–5197.

JM049782N